PERGAMON

International Journal of Heat and Mass Transfer 45 (2002) 3471–3476

International Journal of HEAT and MASS TRANSFER

www.elsevier.com/locate/ijhmt

Technical Note

Stability and chaotic characteristics of a wall plume

Hideshi Ishida [a,*], Takayuki Yamashita [b], Hideo Kimoto [a]

[a] *Division of Mechanical Science, Department of Systems and Human Science, Graduate School of Engineering Science, Osaka University, 1-3 Machikaneyama-cho, Toyonaka, Osaka 560-8531, Japan*

[b] *Hewlett-Packard Solutions Delivery, Ltd., 1-10-11 Ebisu-nishi, Shibuya, Tokyo 150-0021, Japan*

Received 22 August 2001; received in revised form 23 January 2002

Abstract

In this study artificial disturbances were introduced into a wall plume adjacent to a vertical side wall, and its stability and chaotic characteristics were experimentally examined. The main results are: (1) for high and low frequency disturbances the neutral region (a region between stability and instability) is lower and higher values of the modified Grashof number than an analytical neutral curve, respectively. (2) As the Grashof number increases, a chaotic fluctuation of temperature is observed above a critical value. This chaotic region is completely included in the region where the wall plume is unstable. (3) The flow can be classified into four regions based on patterns, a stable region, disturbance-amplification region, chaotic region and non-chaotic region.

Keywords: Natural convection; Wall plume; Chaos; Stability analysis; Non-linear mechanism

1. Introduction

Wall plumes, thermal convection fields induced by heater-embedded or heated side walls, can be regarded as a basic physical model of a buoyancy-driven system, and there have been many investigations into their flow characteristics [1].

Jaluria and Gebhart [2] have analyzed wall plumes arising from a line heat source embedding in a vertical side wall, and Wakitani [3] has numerically examined the stability of these wall plumes as the inclination angle of the wall is changed. Wakitani showed that an upward inclination of a wall stabilizes a wall plume and that the amplification rate of lower-frequency mode, i.e., buoyancy-induced instability mode, is smaller than that of higher-frequency mode. Regarding the latter phenomenon, the numerical study of Dring and Gebhart [4] shows that the amplification rate and propagation speed for higher-frequency disturbances are larger than for lower-frequency disturbances and the wavelength of low-frequency disturbances is much longer than the vertical distance from the leading edge.

An experimental study on the same wall plumes, i.e., arising from a line heat source embedded in a vertical side wall [5], shows that the analytical neutral curve determined by Wakitani [3] can qualitatively explain the measured stability characteristics. However, for a plume induced by a side wall with a constant heat flux the experimentally determined neutral curve [6] is lower in height than an analytically determined one [1,7]. This discrepancy may be due to the assumption of parallel flow as indicated by the analysis of Tanaka et al. [8].

Although the experimental and numerical analyses mentioned above are effective in detecting the onset of unstable flow, they cannot be applied in examining the characteristics of unstable flow fields caused by non-linear mechanisms. Therefore the instability that can be examined in the context of linear stability analysis is not necessarily equivalent to turbulence. From this point of view the chaotic characteristics and their related indicators [9] are of great significance as they provide a quantitative measure by which to examine and classify [10] unstable flow fields, and are very useful for many

* Corresponding author. Tel.: +81-6-6850-6162; fax: +81-6-6850-6163.

E-mail address: ishida@me.es.osaka-u.ac.jp (H. Ishida).

0017-9310/02/$ - see front matter
PII: S0017-9310(02)00058-3

Nomenclature

a	thermal diffusivity (m^2/s)
C_p	specific heat at constant pressure (J/(kg °C))
f	vibration frequency of artificial disturbance (s^{-1})
G	modified Grashof number, defined in Eq. (1)
g	acceleration due to gravity (m/s^2)
k	thermal conductivity (J/(m s °C))
N	proportional constant (°C $m^{3/5}$)
Pr	Prandtl number ($=0.71$)
R	dimensionless range of fluctuation
T	dimensioned temperature (°C)
V	dimensionless variance
x	x coordinate (m)
y	y coordinate (m)

Greek symbols

α	dimensionless amplification factor
α^*	dimensioned amplification factor (m^{-1})
β	dimensionless vibration frequency
β^*	thermal expansion coefficient ($°C^{-1}$)
ΔT	amplitude of temperature (°C)
$\Delta\theta$	dimensionless amplitude of temperature (°C)
Θ	representative temperature difference (°C)
θ	dimensionless temperature ($=(T-T_\infty)/\Theta$)
ε	error band
η	similarity variable ($=Gy/(4x)$)
λ	largest Lyapunov exponent
ν	kinetic viscosity (m^2/s)
τ	time scale at which auto-correlation function becomes $1/e$

Subscripts

inf	infinity, ∞
max	Maximum
min	Minimum
w	wall surface
θ	temperature
+	upper limit
−	lower limit
∞	ambient physical quantity

practical applications. Very little work, however, is available on the relationship between stability and chaos or turbulence [11].

In this study this relationship has been experimentally examined for a vertical wall plume induced by an embedded line heater, and the flow field has been classified on the basis of non-linear effects.

2. Apparatus and procedure

Since natural convection fields such as wall plumes are easily disturbed by environmental forces, a small test room was built in the laboratory for protection from such disturbances. The test room was 3370 mm wide, 3500 mm high and 3440 mm deep. A test box, shown schematically in Fig. 1, and a three-dimensional traverse apparatus were set on a steel table in the test room. The table was placed on an antivibration rubber sheet over the laboratory floor.

The sides of the test box were made of acrylic resin plates 3 mm thick and the front and top of the box were made up of nylon mesh screen sheets for disturbance protection and rectification of the circulation air by natural convection. The bottom of the box was made of a 5 mm thick brass plate, so that the entrainment air was exclusively supplied through the front mesh screen sheet. The back of the box was made of a urea resin plate (1100 mm high, 350 mm wide and 3 mm thick), set upright 180 mm from the front mesh screen and was used as the vertical wall for the wall plume experiment. A nickel–chromium wire of 0.2 mm diameter was embedded

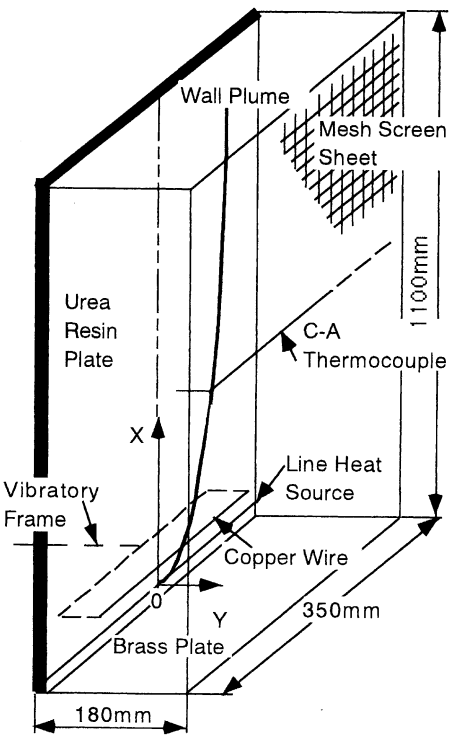

Fig. 1. Test box with mesh screen sheet.

horizontally 5 mm from the bottom of the urea resin plate and was used as the line heat source for the wall plume along the front surface of the plate. The heating rate was fixed at 40 W/m. The wall plume field is indicated in Fig. 1.

An identical line heater was also embedded in the rear side of the vertical wall plate outside the box at a similar place as the line heat source for the wall plume inside the box and its heating rate was set to be the same. As a result, the natural convection fields along the front and back surfaces of the vertical plate were nearly the same, so that the plate was kept in an adiabatic state.

For the analysis of the stability of the natural convection field, a copper wire of 0.2 mm diameter was used to create disturbances in the field. It was set 15 mm above the line heat source embedded in the vertical wall inside the box and was forced to vibrate with a constant amplitude of nearly 1.5 mm by a vibration mechanism driven by a computer-controlled pulse motor. Artificial disturbances of frequencies 0.51, 0.72, 1.0, 1.35 and 2.02 Hz were introduced into the wall plume field. The disturbing frequency was changed by changing the pulse interval to the pulse motor.

A thermocouple made of Chromel–Alumel wires was used of a thermal probe to measure the local temperature. Its nominal diameter of 0.1 mm allowed a thermal time response satisfactory for the present experiment. The thermocouple probe was fixed with a support on a three-dimensional traverse apparatus and the local temperature at any point in the wall plume field could be measured precisely under computer-controlled conditions.

The electromotive force of the thermocouple at each specific point was measured by a computer-controlled digital multimeter for 100 s with a data-sampling frequency of 10 Hz. The voltage data were transmitted to a microcomputer through a GP–IB interface board and the fluctuation characteristics were analyzed.

The results of preliminary experiments showed that the flow field was homogeneous in the lateral direction and sufficiently steady in its laminar region. Hence, the thermal field of the wall plume was examined exclusively in the vertical plane normal to the vertical wall surface through the center of the line heat source. The origin of the coordinate system is located at the center of the line heat source as shown in Fig. 1. The x-axis is vertical, the y-axis is perpendicular to the vertical wall surface, and the z-axis is horizontal to the wall surface.

Moreover, precise measurements of temperature on the x–y plane showed that the fundamental flow characteristics in the laminar (stable) region were in good agreement with the analytical steady-flow solution of Jaluria and Gebhart [2] on which the present stability analysis is based. In the outer region of $\eta \equiv Gy/(4x) > 2$, however, the difference between the local temperature and the ambient temperature remained constant (but not zero), due to both the radiation from the heated surface and the existence of the front mesh screen sheet. The measurement of the present study was, therefore, confined to the region $\eta < 2$.

The test room was closed during the experiment and the three-dimensional traverse apparatus was controlled by a microcomputer outside the test room. During the experiment the temperature in the test room was almost constant in the vertical direction (gradient: 0.5 °C/m) and its fluctuation was confined below the noise level of the thermocouple. Thus, the effects of ambient temperature fluctuation or gradient were negligible.

3. Data analysis

3.1. Evaluation of stability

In this study the stability of the flow at a specific point was experimentally determined by the evaluation of the modified Grashof number G, dimensionless vibration frequency β and dimensionless spatial amplification factor α, defined as follows:

$$G \equiv 4\left(\frac{g\beta^* x^3 \Theta}{4\nu^2}\right)^{1/4}, \quad \beta \equiv \frac{32\pi f x^2}{\nu G^3}, \quad \alpha \equiv \frac{4\alpha^* x}{G}, \tag{1}$$

where Θ, f and α^* are the representative temperature difference $(T_w - T_\infty)$, vibration frequency and spatial amplification factor, respectively. T_w and T_∞ are the local temperature along the x-axis and ambient room air temperature, respectively.

Initially, the thermocouple was traversed along the x-axis in contact with the wall surface. The temperature at the vertical wall surface T_w was measured without any artificial disturbances and the representative temperature difference Θ was evaluated based on the analysis of Jarulia and Gebhart [2]:

$$\Theta = T_w - T_\infty = Nx^{-3/5}, \tag{2}$$

where N is a proportional constant and was calculated by least-square fitting for each temperature distribution in the present study. The dimensionless temperature θ can then be determined from $\theta(x,y) = (T(x,y) - T_\infty)/\Theta(x)$. The room temperature was also used as a reference temperature to evaluate the physical properties. The Prandtl number Pr of the present study was, therefore, held constant at 0.71. Secondly, the change of the amplitude of the temperature fluctuation ΔT over height, evaluated by FFT at the vibration frequency f, was examined by introducing artificial disturbances into the wall plume. The thermocouple was traversed along the curve $\eta = 1.43$, which is defined by the y-direction inflection points of the temperature to ensure a large measured amplitude of temperature. The measurement was iterated 10 times under the same conditions, except

for the case of 2.02 Hz where it was iterated four times. The change of the dimensionless amplitude of temperature $\Delta\theta$ $(= \Delta T/\Theta)$ against x was approximated by a third-order polynomial using least-square fitting. Its 50% error band was also calculated at each measurement point from the unbiased variance around the estimated curve. Using these polynomials and error bands, the upper and lower limits of the dimensionless amplification factor (α_+ and α_-, respectively) were evaluated and the stability at the specific point was determined as follows:

$$\alpha_- > 0: \text{ unstable}, \quad \alpha_+\alpha_- \leqslant 0: \text{ neutral}, \quad \alpha_+ < 0: \text{ stable}. \tag{3}$$

In fact, the amplification factor of the flow cannot remain positive owing to the folding action of non-linear effects, and hence a resultant flow with strong fluctuations in temperature tends to be neutral. This makes it difficult to determine the neutral point or the neutral region of G in the context of linear stability analysis. Therefore once the flow is determined to be unstable through the neutral region with increasing x, its downstream flow was also taken to be unstable.

3.2. The largest Lyapunov exponent

The largest Lyapunov exponent λ was also computed by the method of Wolf et al. [9] from the time-evolution data of temperature when the artificial disturbances were introduced. A dynamic system with $\lambda > 0$ is generally regarded as "chaotic".

Using the method of Ishida and Kimoto [10,11], the parameter values used to compute λ, i.e., the embedding dimension, delay time and evolution time between replacements, were changed, ascertaining that λ was stationary. The ratio of the delay time to the reference time scale τ, at which auto-correlation function becomes $1/e$, was taken as a parameter while the delay time was changed. The uncertainty of the thermocouple, 0.1 °C, was applied to the minimum length of the replacement vector.

When the most suitable parameters were used, any variations in λ were assumed to be merely random error, and λ was evaluated from their mean value in the corresponding range of the parameters. The error band ε_λ was evaluated to be the range of fluctuation with a 50% probability. The temperature measurements were carried out several times under the same conditions and, therefore, the replacement among these data sets can be regarded as an another parameter and the variation of λ with this parameter was also taken into consideration. Using the λ evaluated as above and its error band, the sign of λ is determined as follows:

$$\lambda - \varepsilon_\lambda > 0: \text{ positive}, \quad -\varepsilon_\lambda \leqslant \lambda \leqslant \varepsilon_\lambda: \text{ neutral}, \quad \lambda + \varepsilon_\lambda < 0: \text{ negative}. \tag{4}$$

4. Results and discussion

4.1. Stability of the wall plume

The stability characteristics of a wall plume were determined by the classification scheme given in Eq. (3). The results of this analysis are shown in Fig. 2. In the figure solid circles, plus signs and triangles indicate unstable, stable and neutral, respectively. Solid lines indicate the analytical constant amplification curve of the wall plume adjacent to the vertical side wall [3] and the dashed line is the branch cut which separate the upper high-frequency mode (mode 1) and the lower buoyancy-induced instability mode (mode 2). Comparing the neutral curve ($\alpha = 0$) with the stability characteristics of the present study, it can be seen that the neutral regions for the higher-frequency cases ($f \geqslant 1.0$ Hz) shift slightly to lower values of G. It is assumed that this is due to the non-parallel-flow effect [8]. The lower limit in mode 1 at which there is a frequency component of the positive amplification factor is $G = 50$. The dimensionless time–mean temperature θ_{mean} for various frequencies is shown in Fig. 3(a). Each plotted curve is evaluated as the mean value of all the θ_{mean}'s taken under the same frequency conditions. It can be seen that at the point $G = 50\theta_{\text{mean}}$ begins to increase. This is due to the destabilization of the wall plume, i.e., the enhancement of mixing. The fluctuation around the computed value for $G < 50$ is systematic error caused by the artificial disturbances. To ensure a sufficient accuracy in the evaluated amplification factor and its spatial resolution, however, a sufficient disturbance level is required, as it used in the present study.

For the lower-frequency cases (0.51, 0.72 Hz) the amplification factor is suppressed. This is due to the fact that the propagation speed of a disturbance in mode 2 is

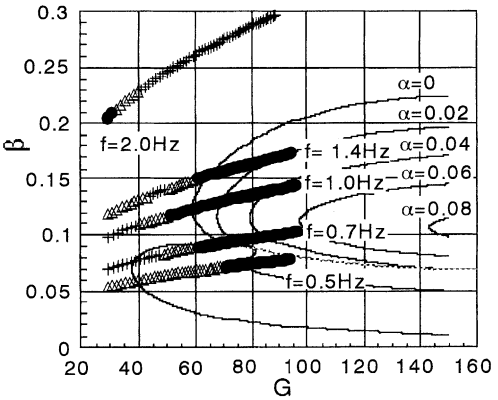

Fig. 2. Stability–instability characteristics of the wall plume: •, unstable; +, stable; △, neutral; –, constant amplification curve, [3]; - -, branch cut [3].

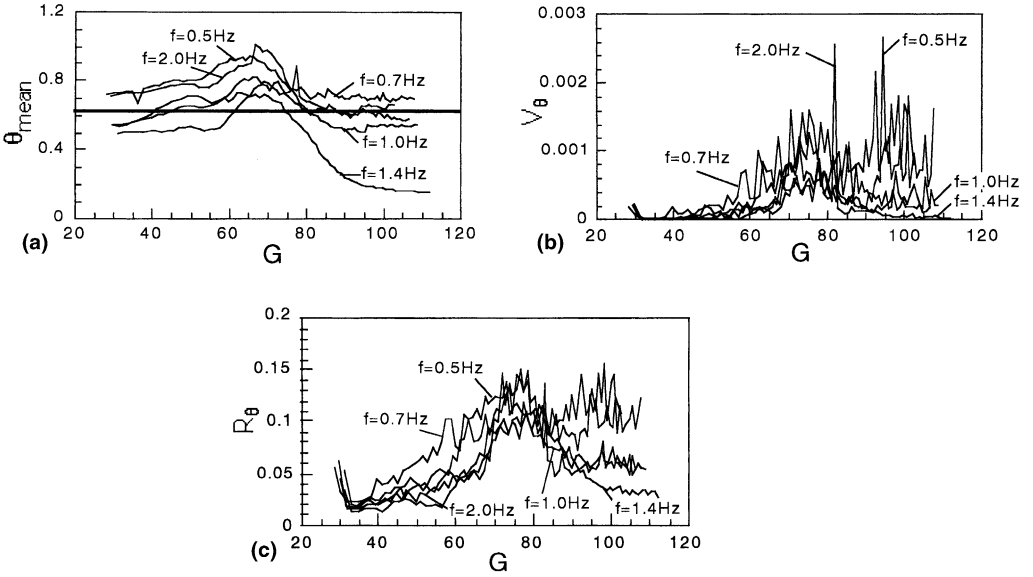

Fig. 3. Thermal response to artificial disturbances: (a) time–mean temperature; (b) variance of temperature; (c) range of temperature fluctuation.

relatively low and its wavelength is much longer than the vertical distance from the leading edge [4].

Neutral or unstable temperature fluctuations are observed even at values of $G < 40$ for the cases where $f > 1.0$ Hz. This is due to the introduced disturbance energy becoming large for higher-frequency cases when the amplitude of disturbance is fixed.

4.2. Chaotic characteristics of the wall plume

Finally, the largest Lyapunov exponent λ was calculated by the method of Wolf et al. [9] from the time-evolution data of temperature when artificial disturbances were introduced. The sinusoidal variation of temperature does not effect the evaluation of λ and, therefore, the disturbance frequency f can be used as the characteristic frequency on G–β space. The results are shown in Fig. 4.

As shown in Fig. 4 the negative λ becomes positive or neutral around $G = 70$ with increasing G. After that the chaotic behavior is weakened and the sign is again reversed to be negative for $G > 85$. This characteristic is independent of its characteristic frequency f. The value $G = 70$ is greater than the above-mentioned lower limit of $G = 50$ in mode 1, hence the chaotic characteristics are related to the amplification of the unstable frequency component of disturbance which is introduced into the wall plume from its surroundings. Herein it should be noted that the region $G > 70$ corresponds to the monotonically decreasing region of θ_{mean} and that the range $70 < G < 85$ corresponds well with the region where the variance of θ, V_θ (see Fig. 3(b)), and the range of temperature fluctuation R_θ ($= \theta_{\max} - \theta_{\min}$, see Fig. 3(c)) becomes large. It follows that these chaotic characteristics are related to the secondary flow, in this case "turbulent flow", caused by non-linear mechanisms to dissipate the fluctuation energy which is amplified by the linear mechanisms. The resultant dissipation of the fluctuation energy causes the flow to become laminar, which is shown by a suppression of the chaotic characteristics for $G > 85$.

The flow region of the wall plume can be classified as follows: (1) stable region ($G < 50$), (2) disturbance-amplification region ($50 \leqslant G < 70$), (3) chaotic region ($70 \leqslant G < 85$) and (4) non-chaotic region ($G \geqslant 85$). Thus the chaotic region of G is included in the unstable

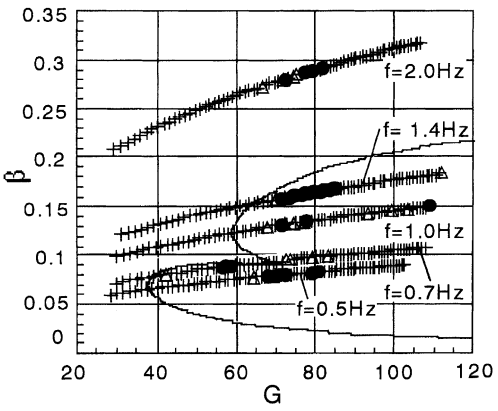

Fig. 4. Chaotic characteristics of the wall plume: •, $\lambda > 0$; +, $\lambda < 0$; △, neutral; –, neutral curve, [3].

region in the context of linear stability analysis and the flow characteristics are strongly affected by non-linear mechanisms in the regions (3) and (4).

5. Concluding remarks

In this study artificial disturbances were introduced into a wall plume adjacent to a vertical side wall and its stability was experimentally examined. Moreover, the largest Lyapunov exponent λ, which is one of the indicators of chaotic characteristics, was calculated and was compared with stability characteristics. The main results are as follows:

(1) In comparison with an analytical neutral curve [3], for the higher-frequency cases a shift to lower values of G of the neutral region is observed which confirms the non-parallel-flow effect shown by Tanaka et al. [8]. For the lower-frequency cases, inversely, a shift to higher values of G of the neutral region is observed which supports the long-wave propagation of disturbances shown by Dring and Gebhart [4].
(2) As G increases, a chaotic fluctuation of temperature is observed over the critical point at which there is a frequency component of the positive amplification factor. At greater values of G the chaotic characteristics are suppressed. This variation can be explained by the generation of secondary flow based on non-linear flow mechanisms and the resultant dissipation of the fluctuation energy.
(3) The flow region of the wall plume can be classified into four patterns, the stable region, disturbance-amplification region, chaotic region and non-chaotic region.

References

[1] B. Gebhart, Natural convection flow, instability and transition, Trans. ASME J. Heat Transfer 91 (1969) 293–309.
[2] Y. Jaluria, B. Gebhart, Buoyancy-induced flow arising from a line thermal source on an adiabatic vertical surface, Int. J. Heat Mass Transfer 20 (1977) 153–157.
[3] S. Wakitani, Instability of a two-dimensional wall plume, J. Phys. Soc. Jpn. 53 (1984) 148–155.
[4] R.P. Dring, B. Gebhart, A theoretical investigation of disturbance amplification in external laminar natural convection, J. Fluid Mech. 34 (1968) 551–564.
[5] H. Kimoto, H. Ishida, H. Ueki, On the thermal field of a wall plume (the response to artificial disturbances), Heat Trans. – Asian Res. 28 (1999) 559–572.
[6] C.E. Polymeropoulos, B. Gebhart, Incipient instability in free convection laminar boundary layers, J. Fluid Mech. 30 (1967) 225–239.
[7] C.P. Knowles, B. Gebhart, The stability of the linear natural convection boundary, J. Fluid Mech. 34 (1968) 657–686.
[8] H. Tanaka, T. Tsuji, Y. Nagano, Stability analysis of thermally-driven flows, in: Proceedings of the 31th National Heat Transfer Symposium, 1994, pp. 232–234 (in Japanese).
[9] A. Wolf, J.B. Swift, H.L. Swinney, J.A. Vastano, Determining lyapunov exponents from a time series, Physica D 16 (1985) 285–317.
[10] H. Ishida, H. Kimoto, The structure of attractors reconstructed with time-evolution data of average heat transfer on thermal convection field in a vibrating square enclosure, Heat Trans. – Asian Res. 30 (2001) 11–21.
[11] H. Ishida, H. Kimoto, Stability and chaotic characteristics of the unsteady flow above horizontal heat sources, in: Proceedings of the 3rd International Symposium on Turbulence, Heat and Mass Transfer, 2000, pp. 307–314.